Phase Entropy-Based Frequency Offset Estimation for Coherent Optical QAM Systems

S. Dris, I. Lazarou, P. Bakopoulos, H. Avramopoulos
School of Electrical and Computer Engineering, National Technical University of Athens, Zografou, GR 15773 Athens, Greece
Author e-mail address: sdris@mail.ntua.gr

Abstract: We investigate a novel approach to Frequency Offset Estimation for coherent optical QAM systems, based on the received symbol phase entropy. It is highly accurate, non-data-aided and oblivious to modulation format.
OCIS codes: (060.0060) Fiber optics and optical communications; (060.1660) Coherent communications

1. Introduction

Frequency Offset Estimation (FOE) is an integral component of the DSP algorithms employed in coherent optical intradyne systems, where the frequency difference between transmitter and local oscillator lasers can be in the GHz range. Popular compensation schemes include those based on the phase increments between successive symbols (e.g. [1,2]), as well as wide-ranging FFT-based algorithms [3]. While FOE based on the symbol phase entropy (PE-FOE) has been presented in [4,5], to the best of our knowledge it has not been explored for photonic communication systems. Here we present a first application of the concept for optical QPSK/QAM, with preliminary results on its performance. Moreover, we modify the basic algorithm to produce a coarse-FOE version that can be used as a preceding stage to reduce overall complexity in a practical implementation.

PE-FOE offers high accuracy and is non-data-aided (NDA). Its most attractive feature, however, is that it requires no a priori knowledge of the transmitted modulation order or constellation shape, making it especially attractive for flexible coherent optical communication systems employing multiple QAM formats.

2. Principle of Phase Entropy-based FOE

In intradyne detection, a data-modulated carrier undergoes complex downconversion by mixing with a local oscillator (LO) in a 90° hybrid. If the carrier frequency ω_c deviates from that of the LO, the resulting baseband signal will contain a residual carrier wave (CW) with frequency $\Delta\omega = \omega_c - \omega_{LO}$. During an observation time T, the probability density function (PDF) of the instantaneous phase (IP), ψ, of this CW signal can be expressed as [4]:

$$p_{cw}^{T}(\psi) = \frac{1}{2\pi}\left[1 + \sum_{l=1}^{\infty} \frac{\sin\left(\frac{l\Delta\omega T}{2}\right)}{\frac{l\Delta\omega T}{2}} b_l \cos(l\psi)\right] \qquad (1)$$

where $b_l = \sqrt{\pi\gamma}e^{-\frac{\gamma}{2}}\left[I_{\frac{l-1}{2}}\left(\frac{\gamma}{2}\right) + I_{\frac{l+1}{2}}\left(\frac{\gamma}{2}\right)\right]$, γ is the signal-to-noise ratio (SNR) and $I(x)$ is the modified Bessel function of order l. Adding modulation to the baseband CW signal, the IP PDF of an M-QAM signal with residual carrier offset $\Delta\omega$ can be determined:

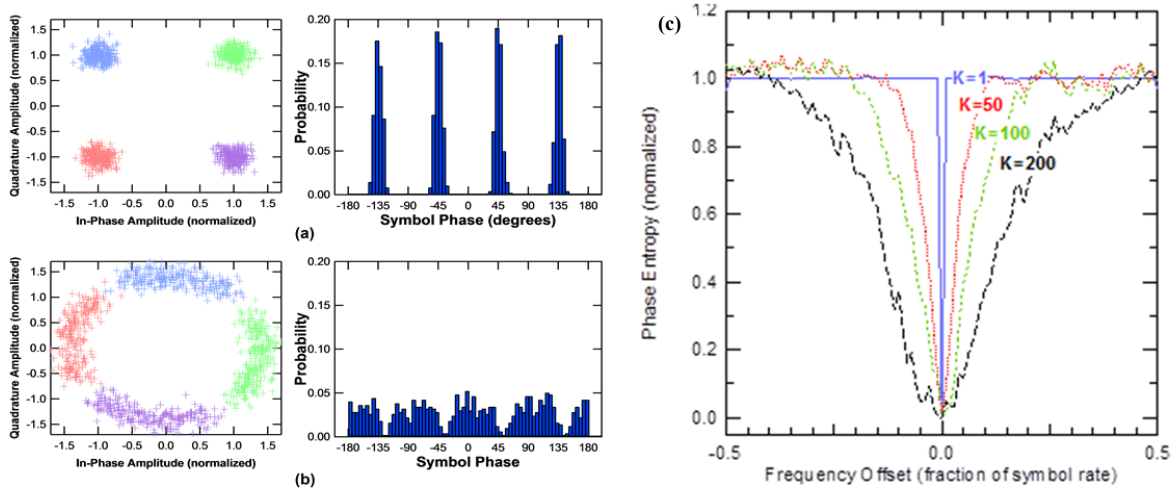

Fig. 1: Illustrating the phase PDFs of a simulated 10Gbaud QPSK signal corrupted by AWGN for (a) no offset, and (b) 20MHz offset. (c) Normalized phase entropy as a function of frequency offset on a simulated QPSK signal, for various values of parameter K (see section 3).

$$p_{mqam}^{\Delta\omega}(\psi) = \frac{1}{M}\sum_{k=1}^{M} p_{cw}^{T}(\psi + \arg\{d_k\} + \Delta\theta) \qquad (2)$$

Where $d_k = a_k + jb_k$ (a_k, $b_k \in \{2m\text{-}1\} : m=1, 2, \ldots \log_2(M\text{-}2)$) are the M-QAM constellation points and $\Delta\theta$ represents the initial phase difference between the data carrier and LO signals. Finally, the phase entropy (PE) can be calculated using Shannon's equation:

$$H_{mqam}^{\Delta\omega} = -\int_{-\pi}^{\pi} p_{mqam}^{\Delta\omega}(\psi) ln\left(p_{mqam}^{\Delta\omega}(\psi)\right) d\psi \qquad (3)$$

A qualitative assessment based on a simple baseband simulation in MATLAB is provided here to illustrate the behavior of Equation (3). Fig. 1 shows 1000 symbols of a noisy 10Gbaud QPSK signal with (Fig. 1b), and without (Fig. 1a) a 20MHz frequency offset. Significant spreading of the symbol phases is evident and this leads to higher entropy for the signal with offset. This is evident in Fig. 1c (see solid line, K=1), where the normalized PE is plotted as a function of frequency offset. The sharp trough exhibited by the PE at zero offset can be exploited for accurate FOE, and forms the basis of our algorithm.

3. Basic Algorithm Description

The proposed algorithm operates on the fourth-power phase information of a block of N symbols. For QPSK this is equivalent to modulation-stripping, while for higher-order QAM constellations it simply wraps the phases within the range $\pm\pi/4$. The motivation behind this approach is twofold: The fourth-power phase operation is ubiquitous in coherent DSP demodulator implementations, as it is used for carrier-phase recovery. Hence, the wrapped phase angles will normally be available anyway, and thus do not represent any additional complexity for the DSP. Secondly, the FOE becomes more accurate than when using the unwrapped phase angles [5].

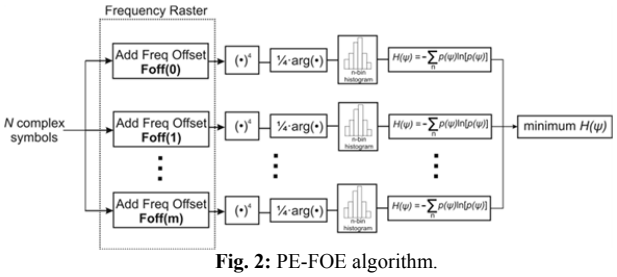

Fig. 2: PE-FOE algorithm.

The basic PE-FOE algorithm is shown in Fig. 2. It is necessary to employ a frequency raster that adds a range of frequency offsets to the baseband data signal. The received complex symbols ($\mathbf{X} = [x_1, x_2, \ldots x_N]^{\mathbf{T}}$) are copied into M paths, each of which receives a corresponding offset given by the M-element vector, $\mathbf{F_{off}}$. The fourth-power phases of each of the resulting vectors are calculated and histogrammed, after which the PE per frequency offset can be determined using Equation (3). The minimum of the PEs then corresponds to the output signal with the least amount of residual frequency offset after the raster. It should be noted that the fourth-power operation in Fig. 2 is placed after the frequency raster, to simplify understanding of the procedure. In practice, the algorithm should be modified to include it before, which avoids having to repeat the operation for every point in the range of frequency offsets.

3. Coarse Estimation

It should be clear from Fig. 1c that the frequency raster must have sufficient granularity so that the trough exhibited by the PE is not missed by the minimum search algorithm. This can introduce unacceptably high complexity due to the need to perform a fine search over the entire range of the FOE (±SymbolRate/8). This can be mitigated by adding a coarse-FOE stage prior to the fine PE-FOE, which in turn can be used for fine adjustment.

Here we introduce a new, simple approach for using PE-FOE as a coarse monitor. The scheme is similar to that employed in [5], but is more robust since it does not require a peak-finding algorithm for the PE PDFs. The main difference with basic PE-FOE is that the block of N received symbols is further subdivided into K subgroups, each having a number of elements L (i.e. $L=N/K$, K being an integer.). The PE is calculated for each one of the K subgroups, and the final estimate is obtained by averaging these together:

$$H_{avg,K} = \sum_K\left[-\sum_L p(\psi)\ln\left(p(\psi)\right)\right]/K \qquad (4)$$

The resulting averaged PE versus frequency offset plots in Fig. 1c show that the trough is expanded (at the expense of accuracy on the estimation) with increasing values of K, hence easing the requirement for fine granularity in the frequency raster. Moreover, it is now possible to use efficient non-linear search algorithms (in place of the linearly-spaced frequency raster) to obtain a rough estimate of the location of the minimum PE.

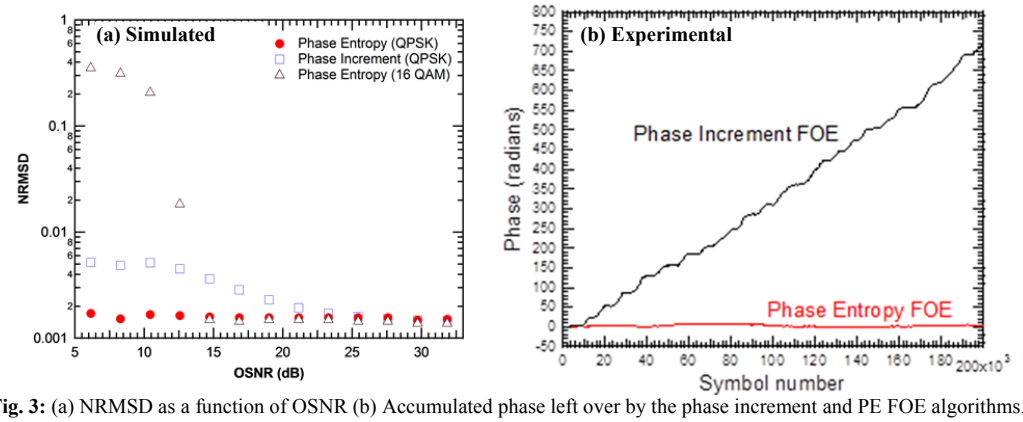

Fig. 3: (a) NRMSD as a function of OSNR (b) Accumulated phase left over by the phase increment and PE FOE algorithms.

4. Simulation

To evaluate PE-FOE for coherent optical systems, a simulation was carried out in VPI TransmissionMaker. A 10GBaud QPSK/16QAM setup with variable OSNR was employed, with the combined linewidth of the Tx and LO set at 1MHz. For each OSNR, 20 simulation runs were carried out, each with random frequency offsets in the range ±1GHz. FOE was performed using the phase entropy over 500 symbols and a fine raster granularity of 0.1MHz, for QPSK and 16-QAM signals. To enable comparison with an existing FOE scheme, the phase increment algorithm described in [1] (for 500 symbols) was also employed for the QPSK case. Fig. 3a shows the Normalized Root Mean Square Deviation (NMSD) of the estimators as a function of OSNR. PE-FOE exhibits superior performance to the phase increment algorithm for lower OSNRs, with the performance of the two estimators converging at higher values. For 16QAM, PE-FOE predictably requires a higher OSNR (~14dB) for satisfactory operation, but for OSNRs >14dB it achieves equivalent results to the QPSK case. This highlights the power of PE-FOE: The exact same implementation of the algorithm can be used for compensation, regardless of modulation format.

5. Experimental Setup

A 22Gbaud QPSK back-to-back intradyne experiment was carried out to verify operation of the PE FOE algorithm in a realistic setting (Fig. 4). A standard unlocked DFB laser with a linewidth specification of <5MHz was used for the transmitter, while a tunable laser with linewidth <1MHz was used as the LO. The baseband I and Q waveforms were captured by a real-time oscilloscope with 50GSa/s ADC sampling rate and 16GHz analog bandwidth. After clock recovery and blind CMA equalization, frequency compensation and carrier phase recovery (CPR) were performed. The latter was used to compare the performance of the phase increment and phase entropy FOE schemes. Any residual frequency offset not compensated by the FOE shows up as accumulated phase in the CPR algorithm. The result is shown in Fig. 3b, where PE-FOE significantly outperforms the phase increment FOE, achieving near zero residual offset and thus confirming that it is an unbiased estimator.

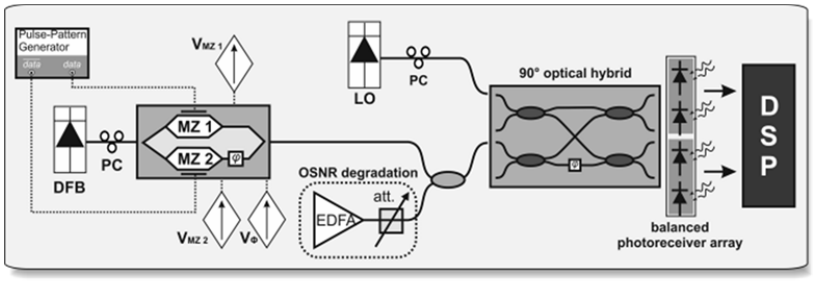

Fig. 4: Experimental QPSK intradyne setup.

7. Conclusion

The first simulated and experimental assessment of phase entropy-based FOE for coherent optical QAM has been presented. We have demonstrated that phase entropy-based FOE is a viable option for photonic communication systems, and is especially attractive for flexible, multi-format coherent receivers.

Acknowledgement: This work was supported by the European Commission through the FP7 project GALACTICO.

8. References

[1] A. Leven, N. Kaneda, U.-V. Koc and Y.-K. Chen, IEEE PTL. **19**, 366-368 (2007).
[2] S. Hoffmann *et. al.*, IEEE PTL. **20**, 1569-1571 (2008)
[3] T. Nakagawa *et. al.*, in ECOC 2010, September 2010, pp. 1-3.
[4] M. Pedzisz and A Coatanhay, IEEE Transactions on Wireless Communications, **5**, 1-5, 2006.
[5] Y. Huang, Q. Yuan and Y. Lu, in IEEE ICC '08, May 2008, pp. 936 – 940.